Supplementary materials

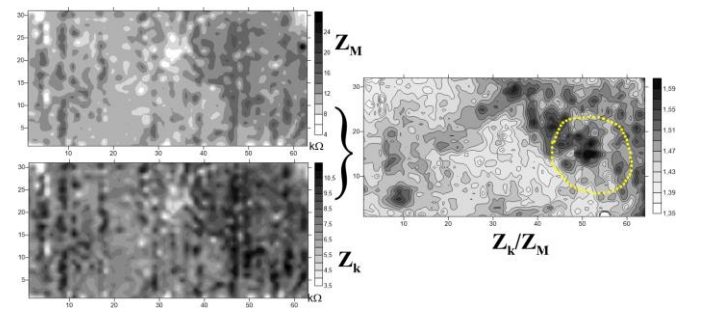

Figure S1. Raw images of the intra- and intercellular impedance module, which show the structural distortions of the primary transducer, and their ratio CDI =$Z_k/Z_{M.}$.

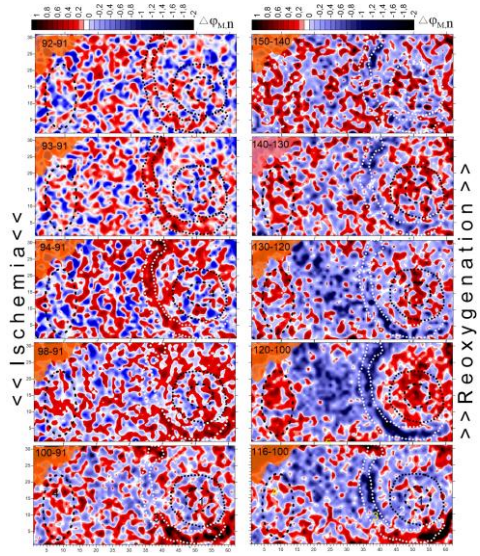

Figure S2. Temporal dynamics of the φ_M landscape during the ischemia-reoxygenation period as difference images. The "3+" structure as a circle begins to form already in the 3rd frame of the ischemia stage. The DS in the center of the frame is clearly emerges and disappears in the reoxygenation stage.

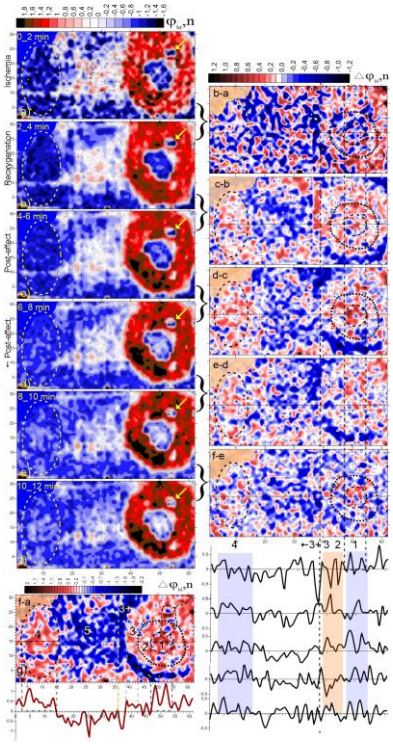

Figure S3. Step-by-step and endpoint changes of φ_M initial landscape during the entire ischemic test. **a,f)** Normalized φ_M-maps averaged over 2-minute periods; **g)** Map of endpoint change. Right: differences of **a-b,b-c,…,f-e.** Bottom: the landscape profiles.
Of note: Contrasting stroma of the PN during **c** and **f.**

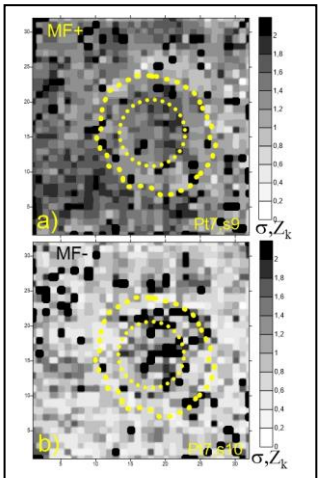

Figure S5. The phenomenon of weakening of fluctuations at the extracellular liquid level (Z_k) in response to the MF turn-over. Dispersion fields (raw maps): **a)** MF↑, b) MF↓.

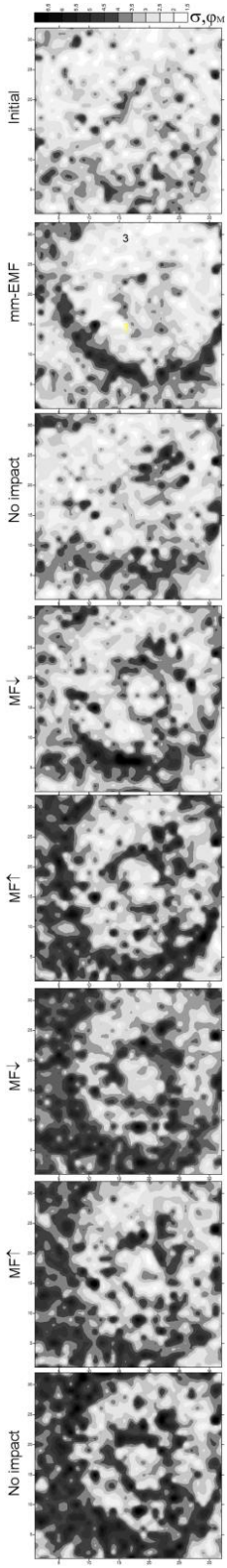

Figure s4. The φ_M spatial fluctuations reveal internal and external boundaries of SSM as the DS structures in response to mm-EMF and MF exposure

Analysis IY. Suspicious nevus[33]

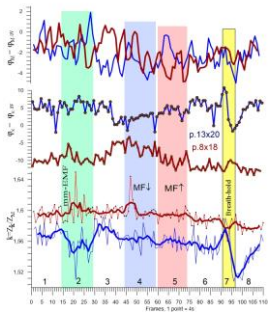

Fig. S12. Counter-directional dynamics throughout the experiment: time graphs of pixels 8×18 and 13×20. Bottom to top: Ionic balance k; deviations of φ_k and φ_M. Of particular note is the phenomenon of locally increased sensitivity of mitochondrial membranes (than those of cell membranes) to EMF/MF exposure, which was also registered in the SSM, Fig. 9.
Notably:
- Antiphaseness of *k* and φ_k in response to mm-EMF and ischemia;
- Antiphaseness and sensitivity of φ_M everywhere only before ischemia with subsequent synchronization only before ischemia followed by φ_M syncronization.

In contrast to the melanoma studies, among 17 nevi examined, there were only 2 cases in which the initial anomalies of the SEL significantly protruded beyond the boundaries of visible tumor. One of them was a papillomatous nevus with finger-like branches, Fig. 1. In the context of DS theory, they can be considered as a pair of extended emitters of negentropy. Unlike local emitters as in the above cases of SM and MSS, the interaction «field» of these emitters will be concentrated between them, thus creating a total asymmetry of the SEL test-induced dynamics. This case was previously presented[33] without analysis – just as an illustration of the antiphase structuring in the suspicious nevus. The experimental protocol was similar to the above, except that breath hold of approximately 40 sec was used as ischemic test, Fig. 12. The following analysis presents this case primarily as an additional experimental proof of the DS phenomena inherent not only in malignant but also in benign neoplasms. At the same time, due to the paucity of such observations, the analysis presented below should be considered just a mechanistic study.

In contrast to melanomas, which exhibit increased cellular disorganization and chaotic growth patterns, benign nevi display a more organized structure relative to surrounding tissues[68]; thus, they can be considered as emitters of negentropy. In this case, papillomatous projections can be considered more powerful entropy emitters due to their altered metabolic states and increased activity levels associated with viral replication. Such cells often exhibit heightened sensitivity to external stressors like EMF and ischemia[69] due to their compromised homeostasis. In contrast, nevi are usually stable lesions with a defined structure that may not respond as dramatically to the external influences.

3.1. Information vs force impact: similarities and differences in coherent structuring

When penetrating host cells, HPV viruses cause changes primarily in cell membranes, which is due to their effect on the activity of ion channels and cellular signaling mechanisms[73].

Fig. 13B shows the initial snap shot landscape in the parameters of cell membranes, φ_k. Dark areas (marked as "2" and "4"), spreading from the visible border of nevus "1" may represent HPV-infected areas[70], i.e. the supposed main emitters of negentropy. To demonstrate similarity of the response of φ_k to the applied stimuli, its dynamics presented as two corresponding columns of correlation fields, Fig.13a,g.

Maps (**a-e**) represent initial stages. The most significant initial dynamics are presented as a complex of (blue) structures "2, 1+,4" surrounding the (red) antiphase zone "3". Exactly the same configuration was restored after the mm-EMF test in (e): only a slight increase in the contrast between the red and blue structures of the complex can be noted after the whole mm-EMF+MF test (stages 2-5, Fig.12). It is also important to emphasize that only a part of the nevus contour stands out in the most contrast, i.e. "1+".

General similarity. In both columns (**b,f**) and (**c,g**), one can see a biphasic response to the stimuli, which, to simplify, can be expressed as "red rising absorbs blue (except "3")" and vice versa:

b,f) The correlation coefficient ***r*** across the entire impedance landscapes increased reaching a value of 1 in **f**, indicating a high degree of order. However, in the projections of the nevus, this coefficient was negative ($-0.66 \le \boldsymbol{r}$ and $-0.38 \le \boldsymbol{r}$, respectively), suggesting localized dysfunction. In this case, the ordering of the surrounding landscape "**f**" occurred with **r** ≈1.0 almost everywhere, whereas in **"b"** – only in "3", i.e. in the area of the emitters focusing area.

c-g) The similarity of both patterns can be defined primarily as the ordering and expansion of the negative coherence zone (up to $-1.0 \le \boldsymbol{r}$) with the destruction of order outside the "2.1+4" sector, which is especially pronounced in the response to ischemia.

(d) The MF-induced destruction of order followed by its recovery in "e".

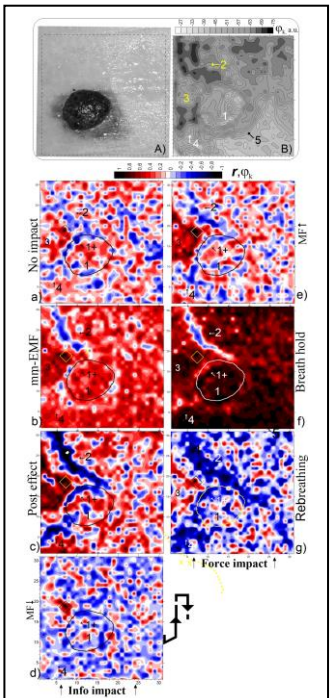

Fig. S13. Information vs force impact on the collective dynamics of cell membranes. **A,B)** Photo of the nevus and a snap-shot of the φ_k landscape; Correlation fields of φ_k landscapes: **a,e)** Initial stages; **b,f)** The mm-EMF exposure and ischemia; **c-g)** Post-effects; **d)** The MF exposure ($p<0.01$).

3.2. Ischemia-induced dynamics and clusterisation

Fig. 14 presents the time-lapse images of emergence, propagation and relaxation of the complex of coherent in-phase and out-of-phase structures at the level of cell membranes during the breath holding and subsequent restoration. The normalized difference images of the φ_k landscape highlight emergence and disappearance of "1+", "2", "3" and "4" structures approximately 8–12 seconds after breathing stops, Fig. 14c. The dynamics of all these structures appear to be synchronous: the blue structures "1+", "2", and "4" appear as a single in-phase ensemble; the red out-of-phase structure "3" located between them, and, only much less pronounced redness, everywhere (including the most of the nevus) on the opposite side of the paired emitters "2" and "4".

The structures "1+" and "3", as in the response to mm-EMF, are located on different sides of the visible border of the nevus thereby opposing *only* its active (viral) part "1+".

Comparing Fig. 14c,d, one you can assess the initial velocity of the red and blue structures of the entire "2-4" complex as 1-2 mm/sec, i.e. similar to that of MS (Fig.2). This value exceeds that observed for calcium wave propagation since the dynamics of ion movement leading to collective membrane depolarization occurs at a higher rate. However, already in the next frame it can be noted that this speed decreased approximately by half (Fig. 14d). In addition, it is noticeable that on the outer side of the emitters "2,1+,4" the speed of propagation of blue structures is noticeably lower.

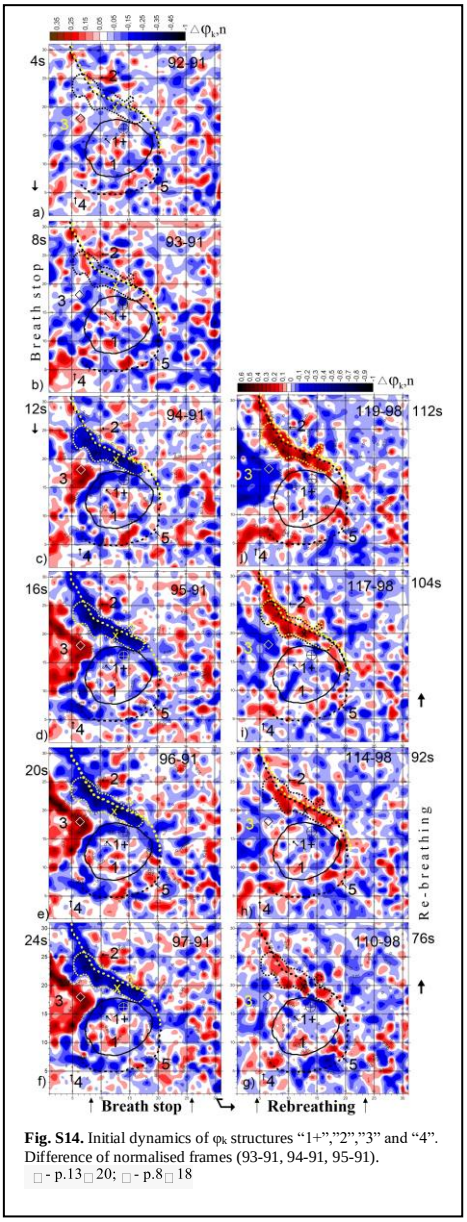

Fig. S14. Initial dynamics of φ_k structures "1+","2","3" and "4". Difference of normalised frames (93-91, 94-91, 95-91).
□ - p.13□20; □ - p.8□18

Delays and abnormalities in intercellular communication during these phases can alter ionic balance within tissues. As signaling cascades unfold over time, variations in ion concentrations (such as Na^+, K^+, Ca^{2+}) across membranes may occur due to differential permeability changes and active transport mechanisms. These alterations can affect conductivity ratios between interstitial fluid and cytoplasm, influencing overall tissue excitability and responsiveness.

Fig. 15 demonstrates restructuring of the ionic balance landscape during the breath-holding period:
- Effect of ischemia on the distribution of the *k* index, where the blue structures can presumably correspond to the HPV infiltration map;
- Time dynamics of three characteristic points of the active zone "1+,2, 3";
- Local changes in *k* in the "2-4" area can exceed the background values by an order of magnitude or more.

The main common feature with the above cases of melanoma is the expansion of functional boundaries in the form of activation and spread of the frontal dynamics of the initial impedance landscape. In particular, it is worth noting the similarity in the following effects and phenomena:
- Ischemia-induced antiphase structuring with propagating wave at the cell membrane level (Fig. 4);
- Ischemia-induced effects of ordering/disordering of fluctuation field of the mitochondrial membrane impedance and advancement of the φ_M functional boundary (Fig. 7);
- Large diversity of temporal response of individual points (Fig. 9); - response to both EMF and hypoxia (Fig. 9);
- (less pronounced, but noticeable) Anomalies in the spatial distribution of ion balance (Fig. 6);
- Increased sensitivity of boundary points to EMF and MF (Fig. 9);
- Dual ordering of the correlation field in response to EMF and MF, characterized by predominance of high positive correlation in the background, juxtaposed with isolated regions/clusters of negative correlation (supposed DS) at the peritumor area, Fig. 11;
- Restructuring of the ionic balance landscape during the breath-hold period, Fig.6f.

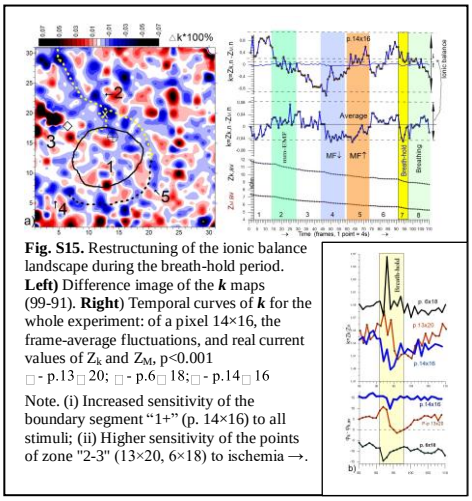

Fig. S15. Restructuning of the ionic balance landscape during the breath-hold period.
Left) Difference image of the ***k*** maps (99-91). **Right**) Temporal curves of ***k*** for the whole experiment: of a pixel 14×16, the frame-average fluctuations, and real current values of Z_k and Z_M, p<0.001
□ - p.13□20; □ - p.6□18;□ - p.14□16

Note. (i) Increased sensitivity of the boundary segment "1+" (p. 14×16) to all stimuli; (ii) Higher sensitivity of the points of zone "2-3" (13×20, 6×18) to ischemia →.

*The observed dynamics can be interpreted through several lenses: o**ncogenic nature of HPV, quorum sensing or viral signalling effect, and** systemic responses following ischemic injury. The transition from positive to negative correlation coefficients can be indicative of malignancy within the nevus and its projections. While these observations do not serve as definitive evidence of malignancy on their own, they align with established principles regarding tumor biology and HPV's role in oncogenesis.*

The dynamics can be also assessed as the initial compensatory mechanism of a two-stage scenario aimed at maintaining cellular integrity and function despite viral interference. In the subsequent phase, however, a pronounced antiphase reaction emerges within these projections, leading to a significant weakening of correlation in the surrounding tissue. The transition indicates a shift from compensatory responses to potential destabilization within the cellular environment. These findings suggest that virus-infected regions act as emitters of negentropy within a DS framework; they disrupt normal cellular function while simultaneously expanding under external stimuli. This duality highlights how pathological entities can exploit environmental pressures for growth despite their detrimental effects on overall tissue homeostasis. Moreover, during this second phase, characterized by the spread of antiphase structures, there is a disturbance of the surrounding landscape, which favors the increase of antiphase islands compared to EMF. This raises intriguing questions regarding underlying mechanisms: Firstly, it may be posited that an increase in the size of negentropy emitters correlates with diminished negentropy flows. Secondly, ischemia appears to exert a more profound influence on the HPV quorum sensing[71] than EMF does, suggesting that cellular communication and collective behavior may be more significantly altered under ischemic conditions.

The rates and delays associated with these two phases are influenced by the number of cells in the ensemble. In larger cell populations, there tends to be enhanced intercellular communication through mechanisms like paracrine signaling or electrical coupling via gap junctions. This can lead to synchronized responses among neighboring cells, potentially speeding up both phases of the response.

Cell biologists study this dynamics using techniques such as e.g. fluorescence microscopy to assess changes in membrane potential or intracellular calcium levels during these phases[72]. DS theory helps explain how these coherent collective responses emerge from individual cell behaviors under external perturbations. The rapid primary response could be viewed as an emergent property arising from local interactions among cells. The slower secondary phase might reflect a transition towards new stable states as cells reorganize their internal structures and functions in response to prolonged stress. The delayed activation of certain pathways may lead to an extended area where coordinated responses occur as neighboring cells begin synchronizing their activities based on restored oxygen levels. This expansion reflects not only recovery but also potential alterations in tumor microenvironments that could influence tumor progression or treatment outcomes.

In conclusion, HPV is the primary cause of cervical cancer, a major global health concern affecting women worldwide. However, current detection methods often lack sensitivity, speed, or cost-effectiveness, especially in resource-limited settings[74]. Our findings elucidate a complex interplay between viral infection and cellular responses within peritumoral papillomatous nevi. The dual-phase reaction underscores critical shifts in cellular dynamics influenced by both ischemic conditions and negentropy considerations. Future research should further explore these mechanisms to enhance our understanding of tumor biology and potential therapeutic interventions.

Analysis V. Antiphase structuring and post-stress effects in a plant leaf*

** New results*

The scanning was performed on a succulent leaf (not separated from the plant) with a time resolution of 8 sec. A drop of laundry bleach was used as a stimulus. Fig. 16c,d shows the primary response to the stimulus in the parameters of the resistive and capacitive resistance of the extracellular environment, i.e. $R=|Z_k|\cos(\varphi_k)$, $Xc=|Z_k|\sin(\varphi_k)$. The difference images demonstrate the instantaneous manifestation of antiphase structures in both parameters around the site of stimulation. However, there are significant differences, of which we will note:

- spatial response in the form of a family of cell membrane mini-clusters (c) is also observed simultaneously in the vessel branching zone «2» due to the fast mechanisms of systemic signalling;
- the response of the extracellular environment (d) is more extensive, but there is an interesting nuance: the outline of this zone (indicated by the dotted line) coincides with the outline of the zone of reduced or zero response (c) (worth comparing with Fig. 3c1,2).

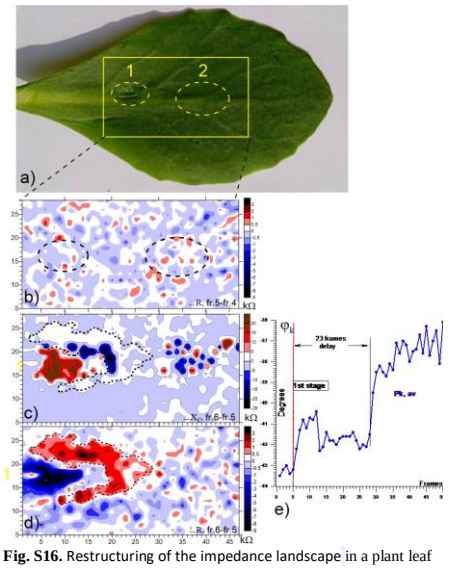

Fig. S16. Restructuring of the impedance landscape in a plant leaf following localized burn and post-stress effect. **a)** Photo of a succulent leaf (still attached to the plant). "1" — burn area, "2" — vessel branching; **b)** Difference map of two frames of the previous frames of the resistive landscape, i.e.fr.5-fr.4 (as seen in e); **c,d)** The first appearance of the response of the extracellular capacitive and resistive landscapes, as fr.6-fr.5; **e)** Time plot of the average phase angle of the extracellular impedance, $p<0.001$.

A description of all the results of this experiment is beyond the scope of this article, but it also seems appropriate to note the phenomenon of a secondary stress response associated with the above-mentioned case of manifestation of the phenomenon of post-ischemic damage (Fig. 5). Fig. 16d shows time graph of the phase angle of the impedance of the

extracellular environment, demonstrating this secondary, significantly more pronounced, systemic reaction that arose approximately 2 min after the end of the local reaction.

This situation can be also analyzed through the lens of DS[36,51]. In plants, when a leaf is irritated, it can trigger a spatial antiphase reaction, where areas of excitation and inhibition occur in a patterned manner around the site of irritation. The spatial antiphase reaction means that energy* is not merely consumed but transformed into organized patterns or structures. When an alkali drop irritates a leaf, it disrupts homeostasis and leads to localized changes in ion concentrations and membrane potentials. This disturbance can create gradients that spread across tissues to maintain order through coordinated reactions in different regions.
*The energy from heat causes denaturation of proteins and disruption of cellular membranes, leading to localized tissue damage and triggering further biochemical responses aimed at repair or defence.

The secondary phase of impedance changes across the entire leaf signifies a systemic response that integrates local damage signals into broader physiological adaptations. This dynamic bears resemblance to stress responses in non-excitable animal cells, where localized injuries also trigger cascades of signaling events leading to alterations in membrane potential and cellular metabolism[55]

In both plant and animal cells, these responses exemplify how living systems utilize electrical properties and biochemical signaling to adapt to environmental stresses while maintaining overall structural integrity.For instance, during ischemia, tissues experience an acute phase where metabolic processes are disrupted, followed by a delayed phase characterized by inflammation and tissue remodeling. This similarity suggests that organisms—whether plants or animals—exhibit common adaptive mechanisms when faced with external stresses. However, while there are overarching principles governing these responses, each type of stress may elicit unique physiological pathways due to differences in tissue structure and function.

Tumors often exhibit heterogeneous responses to therapeutic interventions; understanding how they react to stress can inform treatment strategies, e.g. if tumor exhibits a strong initial antiphase reaction to therapy, it may indicate an immediate defense mechanism that could lead to treatment resistance. Amplitude of the secondary reaction could provide insights into how well tumor adapts over time to therapeutic pressures, potentially guiding decisions on whether to continue or modify treatment protocols. Thus, assessment of these biphasic responses is critically important when considering methods for oncology treatment and tumor reprogrammin[42,56.]